

Larry C. Olsen, F.W. Addis and W.A. Miller  
Joint Center for Graduate Study  
Richland, Washington 99352

#### ABSTRACT

The MINP solar cell concept refers to a cell structure designed to be a base region dominated device. Thus, it is desirable that recombination losses are reduced to the point that they occur only in the base region. The most unique feature of the MINP cell design is that a tunneling contact is utilized for the metallic contact on the front surface. The areas under the collector grid and bus bar are passivated by a thin oxide of tunneling thickness. Efforts must also be taken to minimize recombination at the surface between grid lines, at the junction periphery and within the emitter. This paper includes results of both theoretical and experimental studies of silicon MINP cells. Performance calculations are described which give expected efficiencies as a function of base resistivity and junction depth. Fabrication and Characterization of cells are discussed which are based on 0.2 ohm-cm substrates, diffused emitters on the order of 0.15 to 0.20  $\mu\text{m}$  deep, and with Mg MIS collector grids. A total area, AM1 efficiency of 16.8% has been achieved. Detailed analyses of photocurrent and current loss mechanisms are presented and utilized to discuss future directions of research. Finally, results reported by other workers are discussed.

#### 1. INTRODUCTION

This paper concerns approaches to high efficiency silicon solar cells based on the MINP concept. This term is used to denote shallow junction  $N^+/P$  cells which utilize a MIS contact for the front collector grid. The MINP structure was first discussed by Green, et al.<sup>1</sup> Recently Green and coworkers have fabricated cells exhibiting efficiencies on the order of 19%. As a result, the MINP concept has become one of the most promising approaches to fabricating high efficiency silicon cells.

Key features of MINP cells are described in Figure 1. A shallow emitter is used in an effort to minimize current losses in the emitter region. The front surface is passivated to reduce surface recombination. If the base region losses can be reduced as a result of a back-surface-field, then a  $P^+$  region is established at the back surface. In order that the emitter current losses are further reduced, an MIS contact is used for the front collector grid. A metal must be chosen which will accumulate the  $N^+$  surface. Thus, the area under the front contact is also passivated. Ti and Mg have work functions below 4.0 eV. As a result, these two metals are appropriate for the front tunneling contact. In summary the MINP cell has features similar to other shallow emitter, high efficiency silicon cells. Clearly, the most unique feature is the MIS (tunneling) contact used for the collector grid.

In the next section the theoretical performance of MINP cells will be discussed. Detailed discussions are then given regarding cell fabrication, photocurrent, current loss mechanisms, the Mg/nSi tunnelling contact, and solar cell efficiency.

## 2. LIMITING THEORETICAL PERFORMANCE

Modeling calculations have been conducted to appraise the potential of the MINP concept and to provide guidance for device design. These studies are based on two sources of minority carrier lifetime data, namely, the LSA advisory board<sup>2</sup>, and that of Fischer and Pschunder<sup>3</sup>.

In order to determine an upper limit to cell performance, it was assumed that the device properties were completely determined by the base region. Thus, the junction depth was considered to be vanishingly small and the front surface recombination velocity was set equal to zero. Modeling calculations discussed in this paper are based on an assumed cell thickness of 380  $\mu\text{m}$  (15 mils), since experimental studies have primarily been based on cells with that thickness.

Calculated values of the maximum, active area photocurrent are plotted versus base region resistivity in Figure 2. The modeling calculations were carried out for the two sets of lifetime data and for two conditions at the back contact. An AML irradiance spectrum appropriate for Phoenix, Arizona was used in calculating photocurrent.

Theoretical values of the reverse saturation current ( $J_{B0}$ ) are plotted versus base resistivity and  $N_A$  in Figure 3. Auger recombination and bandgap narrowing are taken into account as done in Reference 1. Calculated values of  $V_{OC}$  are also given assuming  $J_{SC} = 36 \text{ mA/cm}^2$ . With LSA lifetimes, the  $V_{OC}$  for a base region dominated cell can approach 690 mV. Due to Auger recombination, there is no reason to use base resistivities below 0.1 ohm-cm.

Calculated active area AML efficiencies are described by Figure 4. If one assumes that lifetimes are given by LSA values, then a base resistivity in the range of 0.1 to 0.2 ohm-cm is optimum for cells with ohmic contacts, while the resistivity can be any value greater than 0.1 ohm-cm for cells with a BSF. If FP values are assumed, then it is best to use base region resistivities between 0.1 and 1.0 ohm-cm.

## 3. CELL FABRICATION

The basic approaches to cell fabrication involve steps listed in Table 1. To date emitter diffusions have been obtained from ASEC and Spectrolab. The junction depths are on the order of 0.15 to 0.20  $\mu\text{m}$ . Phosphorus concentration profiles obtained by SIMS and spreading resistance analysis (SPA) are shown in Figure 5. The error limits are estimated to be  $\pm 50\%$  for both profiles. Thus, the error limits overlap. Although very limited data has been acquired, it appears that the surface donor concentration is on the order of  $0.5$  to  $1.0 \times 10^{20} \text{ cm}^{-3}$ .

In the case of approach A (Table 1), the wafers are scribed and cleaned, an Al layer is deposited onto the back surface. Heat treatment at 500°C establishes an ohmic contact on the back and a 15 to 20 Å, tunnelable oxide forms on the front surface. This oxide layer provides some passivation on the front surface. Of course, it also serves as an interfacial layer for the MIS, collector grid or 'tunneling' contacts on the front surface. The MIS collector grid is formed with a low work function metal. Mg has been used in this work. Using Approach A, the cell is completed by depositing an AR coating(s).

The key difference with Approach B is that a 100 to 150 Å layer of SiO<sub>2</sub> is grown onto the front surface to achieve a lower surface state density.

#### 4. PHOTOCURRENT

In order to maximize the photocurrent, and to interpret experimental results, detailed analyses of photon and carrier economy have been carried out. In particular, optimum AR structures have been determined for both polished and textured cells. Essential information for such analysis is the internal photoresponse for the cell.

Figure 6 shows a typical result for the internal photoresponse of a polished cell structure. Calculated curves are based on cell parameters as indicated. The wave length region between 750 nm and 1050 nm is the most important one for determining the minority carrier diffusion length. A value of  $L = 150 \text{ } \mu\text{m}$  appears to fit the data fairly well.

Figure 7 describes the approach taken in determining the optimum AR layer structure for polished and textured cells. Optical constants must be known for each layer in the multilayer stack. Photon transmittance into silicon is calculated with a computer code, and used in an integration over the chosen irradiance spectrum. The optimum AR layer structure is determined by maximizing  $J_{PH}$ .

Figure 8 summarizes calculation of  $J_{PH}$  for polished and textured cells. Most of the plots are for  $L = 150 \text{ } \mu\text{m}$ . The active area  $J_{PH}$  is plotted versus  $N_1$ , the index of the antireflecting layer adjacent to silicon. For a single AR case (1L-AR),  $N_1$  is of course the index of the single AR coating. For each value of  $N_1$  in single AR structures, there is an optimum value of the layer thickness. In the case of a two layer structure, there are, of course, optimum value of thickness at which the plotted value of  $J_{PH}$  occurs.

Calculations show that it is desirable to use a textured surface. A single AR coating on top of a textured cell leads to a possible  $38.3 \text{ mA/cm}^2$  compared to the possible  $37 \text{ mA/cm}^2$  achievable with a double AR on a polished surface. Furthermore, with a double AR on a textured surface, a value of nearly  $39 \text{ mA/cm}^2$  becomes possible. Thus results are based on assuming  $L = 150 \text{ } \mu\text{m}$ . If one assumes a Fischer-Pschunder value for  $L$  ( $500 \text{ } \mu\text{m}$ ), a value of  $42.5 \text{ mA/cm}^2$  becomes a possibility.

Table 2 indicates some of the best active area values of  $J_{PH}$  measured by SERI. Those values are fairly compatible with results given in Figure 8. It would appear that the diffusion length of the material used by Green and coworkers is slightly larger than  $150 \text{ } \mu\text{m}$ . The JCGS result of  $37.8 \text{ mA/cm}^2$  for a textured/1L-AR case is slightly less than the possible  $38.2 \text{ mA/cm}^2$ , probably due to absorption. The Spire result may be due to a smaller diffusion length or absorption in the AR coating.

#### 5. CURRENT LOSS MECHANISMS

Current-voltage characteristics are being studied in detail in order that limiting current mechanisms can be identified and understood. Figure 9 summarizes the theory for the current loss mechanisms under consideration. Temperature dependent current-voltage characteristics are particularly useful for determining I-V mechanisms. The activation energy coupled with the n-value and magnitude of  $J_0$  can often suggest the operative current loss mechanism. Table 3 lists the range of values for key I-V parameters.

The emitter recombination current is likely to be a dominant loss mechanism in low resistivity devices. Calculated values of  $J_{0E}$  are plotted vs the surface donor concentration ( $N_s$ ) in Figure 10. The work of Fossum and Shibib<sup>4</sup> was used to calculate  $J_{0E}$ . The effects of bandgap narrowing and of the low lifetime in the emitter are taken into account. Values of  $J_{0B}$  are indicated assuming LSA and FP lifetimes, as well as ohmic and BSF conditions for the back contact. In addition, values of  $V_{OC}$  calculated assuming  $J_{SC} = 36 \text{ mA/cm}^2$  are given. The estimated value of  $J_0$  for the 19% cell of Green, et al is based on the assumption that  $n = 1$ .

I-V data are taken with a computer based data acquisition system over a range of temperatures and under both dark and illuminated conditions. The approach to data analysis is summarized in Figure 11. The approach used for analyzing illuminated data is similar. In general, we observe two current mechanisms, one dominant at low voltages and one dominant at higher voltages. These current mechanisms are referred to as the lower and upper mechanisms, respectively.

Transformed I-V characteristics for an MINP cell are shown in Figure 12. The two mechanisms are clearly evident. Values for the  $J_0$  and  $n$  of the upper mechanism, and  $J_0$  and  $B$  of the lower mechanism were determined for each temperature. Results are typically obtained for ten temperatures. The value of the upper mechanism is plotted versus  $1000/T$  in Figure 12. From this plot, one obtains a value for  $\phi = 1.08 \text{ eV}$ . In analyzing the temperature dependent data,  $J_{00}(T)$  is assumed to vary with temperature as  $\exp(-(T-T_0))$ , with  $T_0 = 100^\circ\text{K}$ .

Some results of I-V analyses carried out for MINP cells are given in Table 4. In particular, the results for the upper mechanism are given. The lower mechanism is discussed below. Results for analysis of both illuminated and dark data are given. Only results of I-V analyses were included, for which temperature studies were made, except for cells 84-21 and 84-22. These devices were made just recently. Consider cell 83-25. Since  $n = 1$ , and  $\phi = 1.08 \text{ eV}$ , it appears that the current-voltage characteristics are limited by the emitter current with bandgap narrowing of  $\Delta E = 0.12 \text{ eV}$ . In all of the other cases,  $n$  is in the range of 1.04 to 1.09, and  $\phi$  lies in the range of 0.7 to 0.8 eV, except for cell 84-5. These parameters suggest either depletion region recombination or field emission. Further study is required to allow one to choose between these possibilities, and to relate the results to processing. It is not clear at this time what is the proper model for 84-5.

The upper mechanism is usually described by  $n \approx 1.0$  to 1.07 and  $J_0 \approx 2 \times 10^{-12} \text{ A/cm}^2$ . At this point it would appear that recombination in the depletion region or field emission by holes near the metallurgical junction explain the upper mechanism. A possible reduction of the magnitude of this mechanism may be accomplished by reducing  $N_s$ .

The lower mechanism is not presently limiting cell performance. It could do so in the future, as the upper mechanism is improved. Thus, we must eventually understand the lower mechanism.

## 6. Mg/n-Si TUNNELING CONTACT

The MIS collector grid is a key feature of the MINP cell. The term 'tunneling contact' is often applied to this contact and will be used in this paper. Figure 13A illustrates the expected electron band diagram at the Mg-nSi interface. Since the work function of Mg is less than 4.0 eV, the silicon surface is accumulated as shown. Majority carriers can readily tunnel through the 20 Å interfacial layer, thus providing a good ohmic contact.

The primary purpose for using a tunneling contact is to minimize the recombination under the contact. Thus, it is of interest to estimate the surface recombination velocity for this interface. We will examine this question in two ways. First, it is informative to investigate MIS diodes on p-type silicon. Figure 10B indicates possible common current loss mechanisms. Mg/pSi MIS cells have been fabricated and found to have excellent properties. Figure 14 shows I-V characteristics for two devices. Device 82 MgSi-14 shows a rather weak lower voltage mechanism, while the more recently fabricated device 84 MgSi-1 exhibits essentially no lower mechanism. More significantly, the upper mechanism for 84 MgSi-1 corresponds to an ideal diode. The I-V parameters are  $n = 1.00$  and  $J_0 = 4.8 \times 10^{-13} \text{ A/cm}^2$ . This value of  $J_0$  can be interpreted in terms of a barrier height of  $\phi_{BF} = E_g$  and  $A = 32 \text{ a/cm}^2$ . Thus, one can conclude that in the case of an Mg/pSi contact, there is no significant surface recombination (c), or tunneling/recombination (d).

The I-V analyses of MINP cells can provide information about surface recombination under the Mg contact on  $N^+/P$  structures more directly. The Mg contact area is not the same for the cells listed in Table 4. Referring to cells 84-21 and 84-22, the Mg contact area differs by a factor of 20. Yet the  $J_0$  is very similar for the two devices. In fact,  $J_0$  for 84-21 is larger than for 84-22. If recombination under the Mg contact were the dominant loss mechanism for 84-22, the  $J_0$  should be smaller for a device with the contact covering less area.

More effort will be devoted to characterize recombination under the MIS contact. However, recombination losses appear to be low enough to allow  $J_0$  to decrease below  $10^{-12} \text{ A/cm}^2$ .

## 7. CELL EFFICIENCIES

Two types of cell structure are being pursued, namely: an MINP configuration with a polished front surface; and MINP cells with textured front surfaces. These structures will be referred to as 'polished' and 'textured'.

The best result obtained with a polished cell is described by Figure 11. The current-voltage characteristics were measured by SERI. As noted, the efficiency was 15.6%, and  $V_{OC} = 636 \text{ mV}$ . This cell utilized a single AR layer of SiO. The SiO is deposited rapidly so that the index of refraction is near 1.9. Analysis indicates that a silicon homojunction with a single AR layer can provide an active area AMI photocurrent of  $35.5 \text{ mA/cm}^2$ . The total area current in such a case for our cells would be  $33.4 \text{ mA/cm}^2$  (6% shadowing). The best total area value of  $J_{SC}$  obtained for a cell with a single SiO layer is  $31.8 \text{ mA/cm}^2$ . Thus, it appears that approximately  $1.6 \text{ mA/cm}^2$  are lost due to photon absorption in the SiO film. Future efforts will concentrate on the use of a double AR coating on a polished cell structure.

SERI measured current-voltage characteristics for the best textured cell are given in Figure 16. Although  $J_{SC}$  has been increased to  $35.5 \text{ mA/cm}^2$ , FF and  $V_{OC}$  are slightly lower than that achieved with a polished cell. Part of this decrease is due to the fact that the junction area of the textured cell is larger than the standard cell by a factor of 1.7, but most of the effect is primarily because the junction has not been optimized for the textured cells.

## 8. CONCLUSIONS

The MINP cell structure is a shallow emitter cell structure. The unique feature of the MINP cell is the tunneling contact used for the collector grid. Like any shallow emitter cell, the front surface must be well passivated and emitter losses minimized before base limited performance can be achieved. Efficiencies of 25% should eventually be possible. Figure 17 indicates the kind of property improvements needed to achieve 20%, and then 25%.

## ACKNOWLEDGEMENTS

The authors wish to acknowledge the financial support of the Solar Energy Research Institute(Contract XBB-2-02090-5).

## REFERENCES

1. M. A. Green, et al, "The MINP Solar Cell - A New High Voltage, High Efficiency Silicon Solar Cell," Conf. Record, 15th IEEE Photovoltaics Specialists Conf., Orlando, p. 1405, 1981.
2. M. Wolf, "High Efficiency Silicon Solar Cells," Conf. Rec., 14th IEEE Photovoltaics Specialists Conf., San Diego, p. 674, 1980.
3. H. Fischer and W. Pschunder, "Impact of Material and Junction Properties on Silicon Solar Cell Efficiency," Conf. Rec., 11th IEEE Photovoltaics Specialists Conf., Scottsdale, p. 15, 1975.
4. Jerry G. Fossum and M. Ayman Shibib, IEEE TRANS ON ELEC. DEV ED-28, 1018(1981).

TABLE 1

### MINP CELL FABRICATION

#### A. WITH THIN PASSIVATING OXIDE

1. Diffuse Emitter into Wafer.
2. Scribe into 2 cm x 2 cm Substrates.
3. Clean Substrate (Basically RCA Process).
4. Deposit Aluminum Back Contact.
5. Sinter Back Contact at 500 C and Grow 15 to 20 A Tunnelable Oxide on Front Surface
6. Deposit Collector Grid Based on a Tunneling Contact.
7. Deposit an AR layer(s).

#### B. WITH THICK PASSIVATING OXIDE

- 1,2 and 3 Same as Above.
4. Grow 100 to 150 A SiO<sub>2</sub> Layer for Passivation of Front Surface.
5. Define Contact Openings and Remove Oxide on Back Surface.
6. Complete cell by Using Steps 4 Through 7 Given Above.

TABLE 2  
EXPERIMENTAL RESULTS FOR AM1 PHOTOCURRENT

**0.2 Ohm-cm P-TYPE BASE  
CELL THICKNESS = 15 mils**

CELL	AR STRUCTURE	GRID SHADOWING	TOTAL AREA AM1 J <sub>PH</sub>	ACTIVE AREA AM1 J <sub>PH</sub>
GREEN, ET AL	2L-AR ZnS/MgF <sub>2</sub>	4.2%	36.0	37.6
SPIRE	TEXTURED 1L-AR(Ta <sub>2</sub> O <sub>5</sub> )	3-4%	36.1	37.2-37.6
JCGS 84-6	TEXTURED 1L-AR(SiO <sub>2</sub> )	6%	35.5	37.8

TABLE 3  
KEY PARAMETERS FOR CURRENT MECHANISMS

CURRENT MECHANISM	J-V RELATIONSHIP FOR V >> kT	ACTIVATION ENERGY φ (eV)
EMITTER RECOMBINATION	$J_{OE} \exp(V/nkT)$ n = 1	1.2 - (ΔE) EMITTER BGN
BASE REGION RECOMBINATION	$J_{OB} \exp(V/nkT)$ n = 1	1.2 (ΔE) BASE BGN
DEPLETION LAYER RECOMBINATION	$J_{OR} \exp(V/nkT)$ n ≅ 1 TO 2	E <sub>c</sub> - E <sub>t</sub> OR E <sub>t</sub> - E <sub>v</sub>
FIELD EMISSION	$J_{OF} \exp(CV)$ $C = \frac{1}{nkT} + B$	0.8 TO 1.0
TUNNELING	$J_{OT} \exp(BV)$	TYPICALLY 0.1 TO 0.2

ASSUMED FORM OF J<sub>oi</sub>:  
 $J_{oi} = J_{oo}(T) \exp(-\phi/kT)$



TABLE 4

## I-V PARAMETERS FOR HIGH-VOLTAGE CURRENT-LOSS MECHANISM

CELL	FRONT Mg CONTACT AREA (%)	DARK OR ILLUM	AVERAGE ERROR FOR UPPER RANGE (%)	UPPER MECHANISM:		
				ACTIVATION ENERGY, $\phi$ (eV)	n	$J_0$ (A/cm <sup>2</sup> )
83-22	6	ILLUM	0.19	0.73	1.04	2.1 E-12
83-23	6	DARK	0.19	0.77	1.09	1.5 E-11
83-25	6	DARK	0.63	1.08	1.00	2.2 E-12
83-26	6	DARK	0.28	0.81	1.04	4.4 E-12
84-5	0.6	DARK	0.19	1.15	1.04	2.4 E-12
84-6	6	DARK	0.33	0.80	1.07	2.4 E-11
84-21	0.3	ILLUM	0.40	—	1.09	5.3 E-12
84-22	6	ILLUM	0.40	—	1.05	2.6 E-12

TABLE 5

## EXPERIMENTAL RESULTS FOR MINP CELL AM1 EFFICIENCIES

0.2 Ohm-cm P-TYPE BASE  
CELL THICKNESS = 15 mils

CELL	METAL USED FOR MIS CONTACT	AR STRUCTURE	GRID SHADOWING	$J_{sc}$ (mA/cm <sup>2</sup> )	$V_{oc}$ (mV)	FF	AM1 EFFICIENCY (%)
GREEN, Et al	Ti	2L-AR ZnS/MgF <sub>2</sub>	4%	36.0	650	0.812	19.0
JCGS 84-4	Mg	2L-AR SiN/SiO <sub>2</sub>	6%	31.1	636	0.787	15.6
JCGS 84-6	Mg	TEXTURED 1L-AR(SiO <sub>2</sub> )	6%	35.5	617	0.768	16.84

Results for Green, et al, were reported at the IEEE 16 th Photovoltaic Specialists Conference.

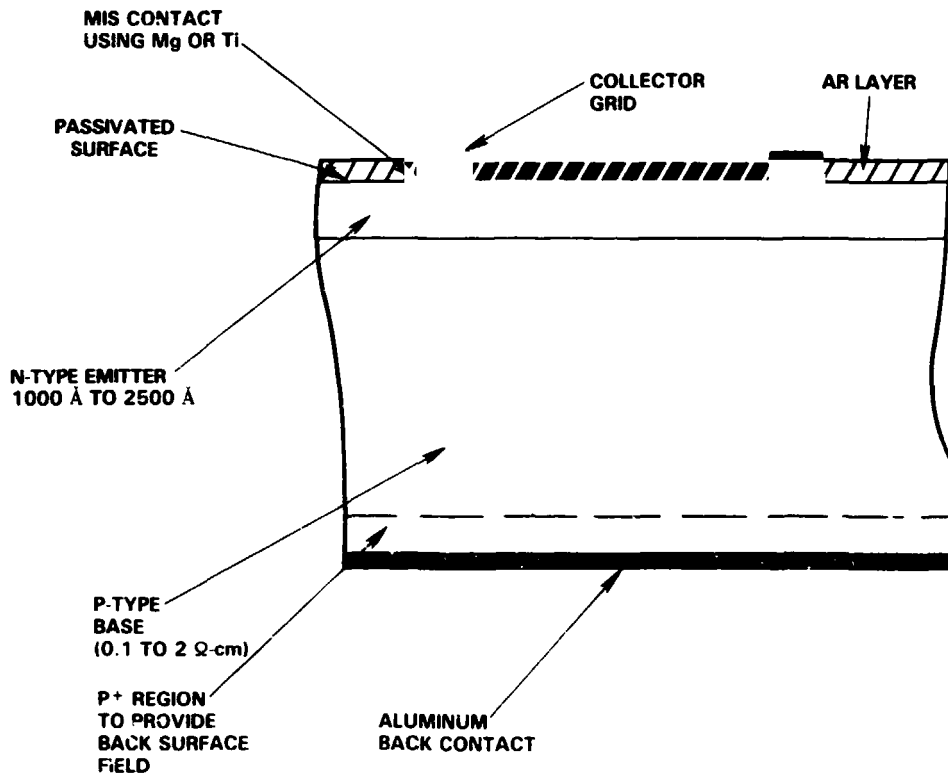


Figure 1. MINP Solar Cell Concept.

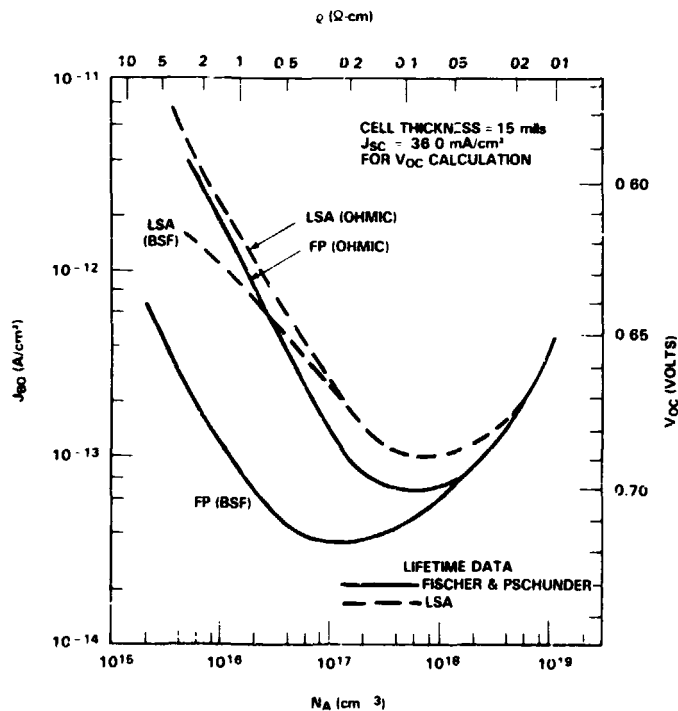


Figure 2. Base Region Contribution to  $J_0$  vs Acceptor Concentration for 15 mil Cell Thickness.

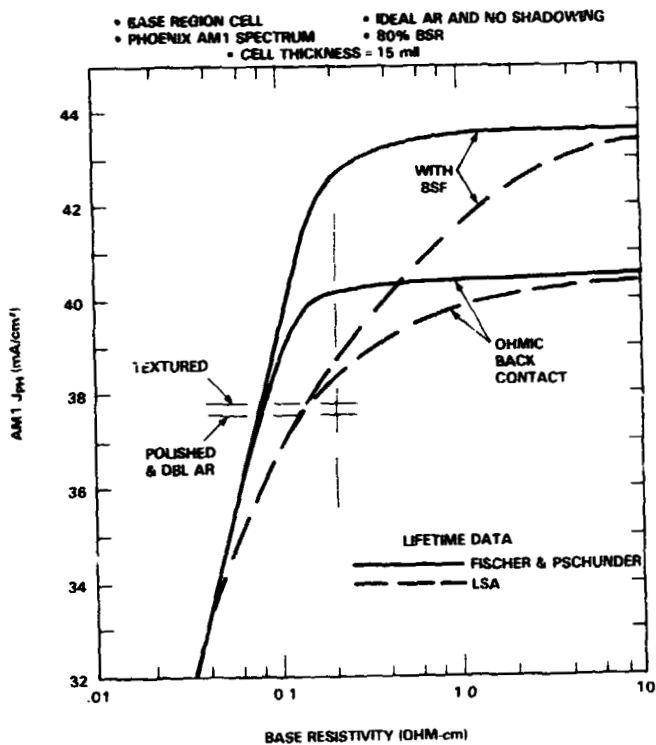


Figure 3. Calculated AM1  $J_{ph}$  vs Base Resistivity for 15 mil Cell Thickness, Assuming 100% Photon Transmittance And No Grid Shadowing.

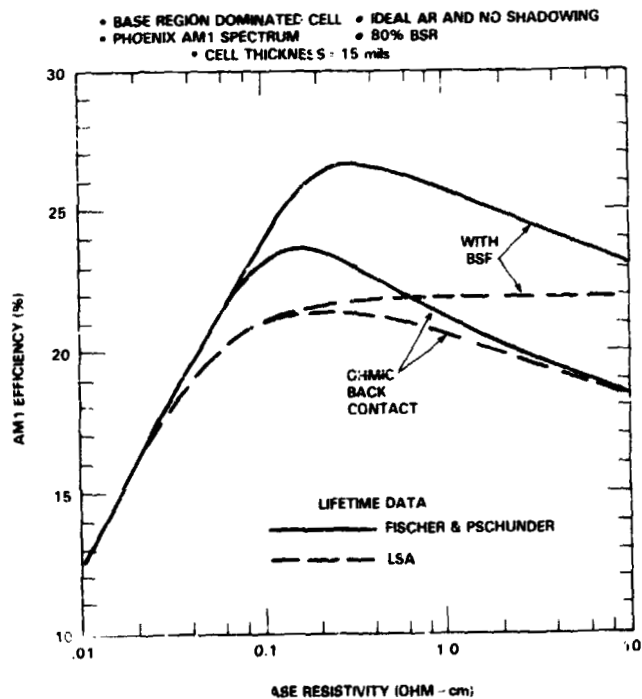


Figure 4. Calculated AM1 Cell Efficiency For 15 mil Cell Thickness, Assuming 100% Photon Transmittance And No Grid Shadowing.

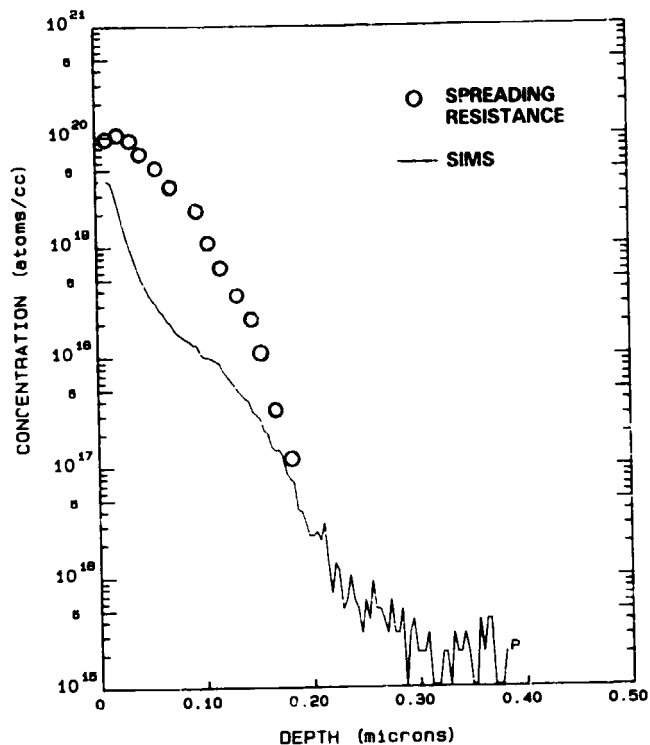


Figure 5. Phosphorus Concentration vs Depth For MINP Cell.

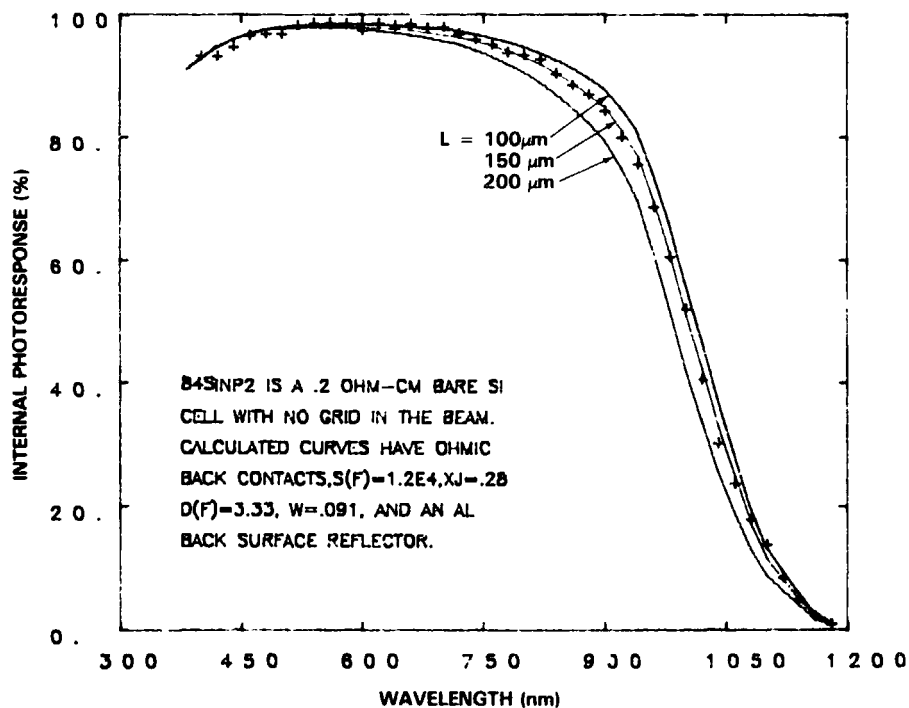


Figure 6. Internal Photoresponse For MINP Cell.

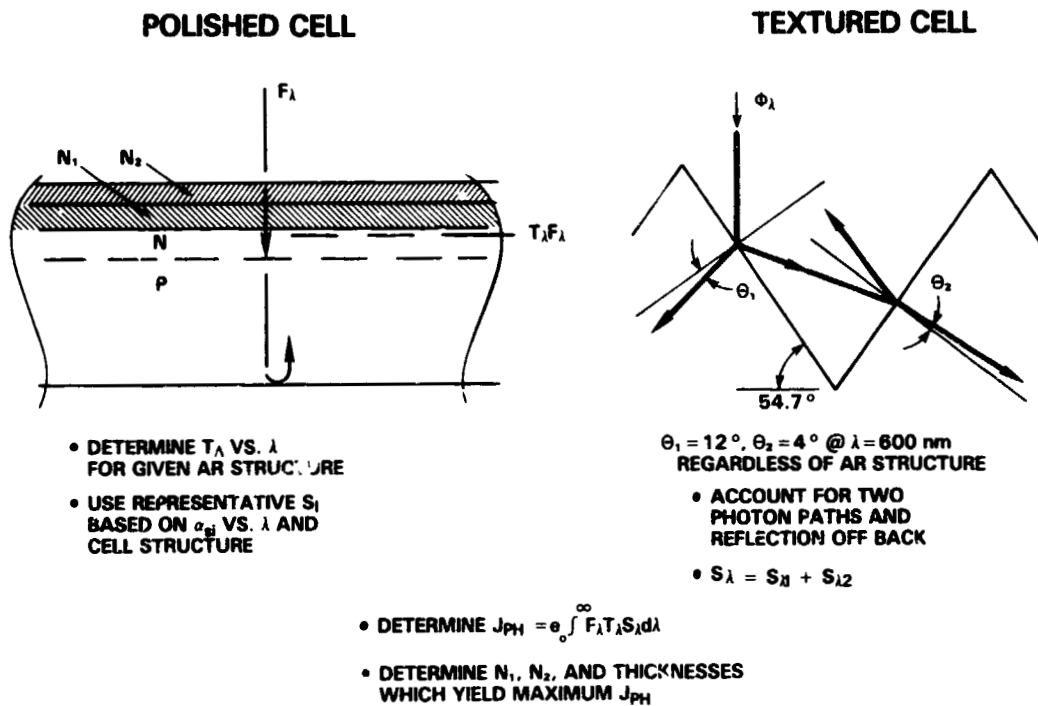


Figure 7. Description of Approach to Optimum AR Layer Analysis.

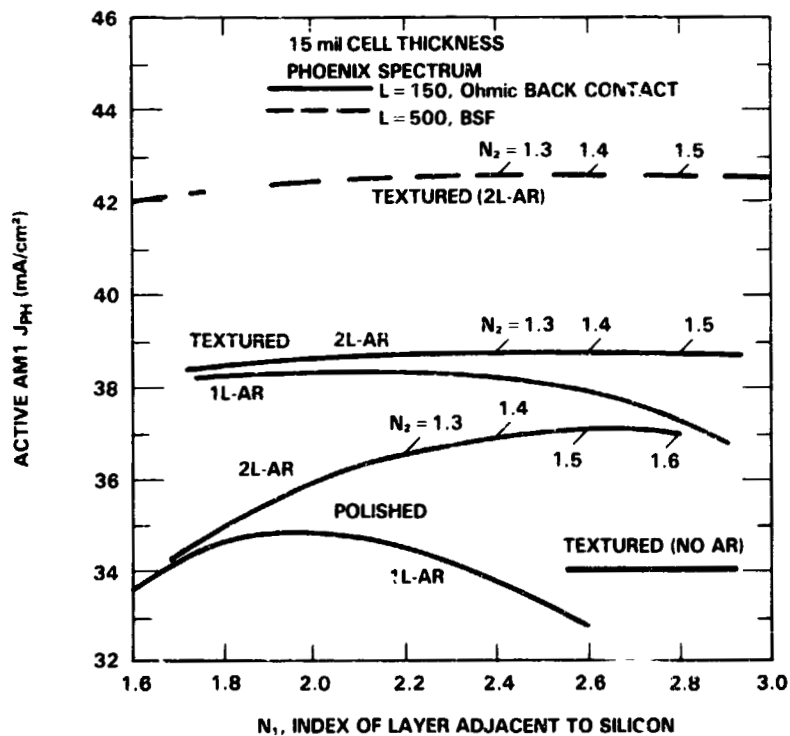


Figure 3. Calculated  $J_{PH}$  vs  $N_1$ , The Index Of The AR Layer Adjacent To Silicon, For Polished And Textured Cells.

### 1. EMITTER RECOMBINATION CURRENT

$$J = J_{OE} \left( \exp\left(\frac{V}{nkT}\right) - 1 \right)$$

$$n = 1$$

FOR RM TEMP ANALYSIS:

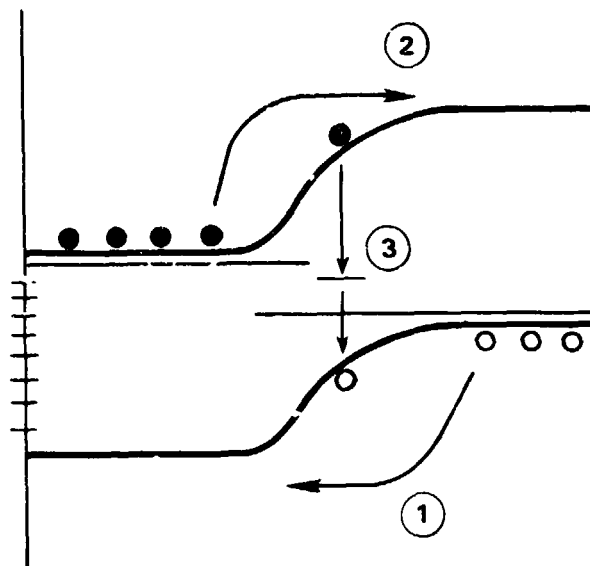
$$J_{OE} = \frac{qn^2}{N_D(\text{EH})} \cdot GF$$

GF IS A FCT OF  $W_H$ ,  $S_p$ ,  $D_{pO}$  &  $\tau_p$

FOR INTERPRETATION OF TEMPERATURE DEPENDENT DATA:

$$J_{OE} = J_{OO}(T) \exp\left(\frac{-\phi}{kT}\right)$$

$$\phi = 1.20 - (\Delta E)_{\text{EMITTER BGN}}$$



### 2. BASE REGION RECOMBINATION CURRENT

$$J = J_{OB} \left( \exp\left(\frac{V}{nkT}\right) - 1 \right)$$

$$n = 1$$

$$J_{OB} = \frac{qn^2}{N_A} \frac{L_n}{\tau_n} \cdot G_F$$

$$= J_{OO}(T) \exp\left(\frac{-\phi}{kT}\right)$$

$$\phi = 1.20 - (\Delta E)_{\text{BASE RGN}}$$

### 3. DEPLETION LAYER RECOMBINATION CURRENT

$$J = J_{OR} \exp\left(\frac{V}{nkT}\right) \quad V \gg kT$$

$$J_{OR} = J_{OO} \exp\left(\frac{-\phi}{kT}\right)$$

$$\phi = (E_t - E_v) \text{ OR } (E_c - E_t) \quad n = 1 \text{ TO } 2$$

$$\text{FOR } n \approx 2, \phi \approx E_g/2 \quad \text{FOR } n \approx 1, \phi \approx 0.8 \text{ eV}$$

### 4. TUNNELING/RECOMBINATION

$$J = J_{OT} \exp(BV) \quad V \gg kT$$

B TEMPERATURE INDEPENDENT

$$J_{OT} = J_{OO} \exp\left(\frac{-\phi}{kT}\right)$$

$\phi$  TYPICALLY 0 TO 0.5 eV

### 5. FIELD EMISSION

$$J = J_{OF} \exp(CV)$$

$$C = \frac{1}{nkT} + B$$

$$J_{OF} = J_{OO} \exp(-\phi/kT)$$

$$\phi = fV_{bi} \quad f = n^{-1}$$

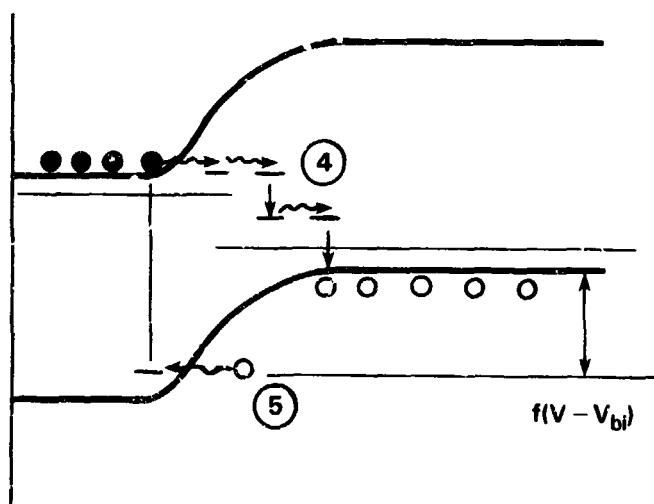


Figure 9. Summary Of Theory For Current Loss Mechanisms.

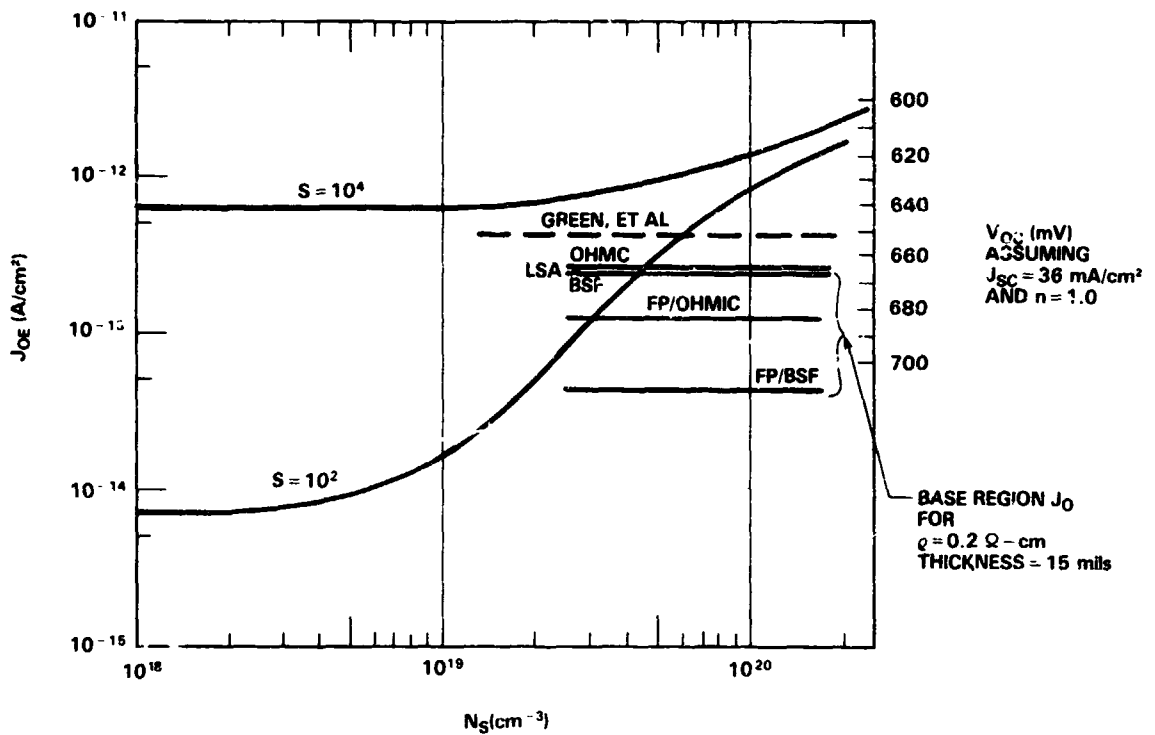


Figure 10.  $J_{OE}$  vs Surface Donor Concentration ( $N_S$ ) For Range Of Values of Surface Recombination Velocity.

#### I-V RELATIONSHIP ( $V_j \gg kT$ )

$$I_{MEAS} = I_j + V_j/nkT$$

$$V_j = V_{MEAS} - R_s I_{MEAS}$$

$$I_j = I_{o1} \exp(BV_j) + I_{o2} \exp(V_j/nkT)$$

#### FITTING PROCEDURE

1. SELECT  $R_s$  AND  $R_{SH}$
2. GENERATE ( $I_j$ ,  $V_j$ )
3. CONSIDER ( $I_j$ ,  $V_j$ ) FOR REGION 1

$$I_j = I_{o1} \exp(BV_j)$$

$$\log_e(I_j) = \log_e(I_{o1}) + BV_j$$

$$\text{LEAST SQUARES FIT} \Rightarrow I_{o1}, B$$

4. CONSIDER ( $I_j$ ,  $V_j$ ) FOR REGION 2

$$I_{j2} = I_j - I_{o1} \exp(BV_j)$$

$$= I_{o2} \exp(V_j/nkT)$$

$$\text{LEAST SQUARES FIT} \Rightarrow I_{o2}, B$$

5. ITERATE BETWEEN REGIONS 1 AND 2 UNTIL ACHIEVE CONVERGENCE.
6. CARRY OUT STEPS 1 THROUGH 5 FOR ARRAY OF  $R_s$  AND  $R_{SH}$  VALUES. SELECT VALUES OF PARAMETERS WHICH PROVIDE BEST FIT TO DATA.

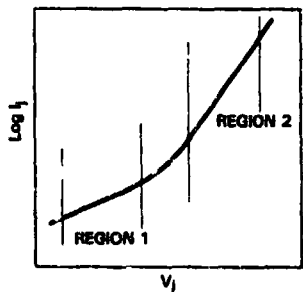
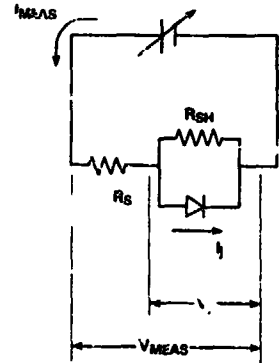


Figure 11. Approach To Dark I-V Analysis.

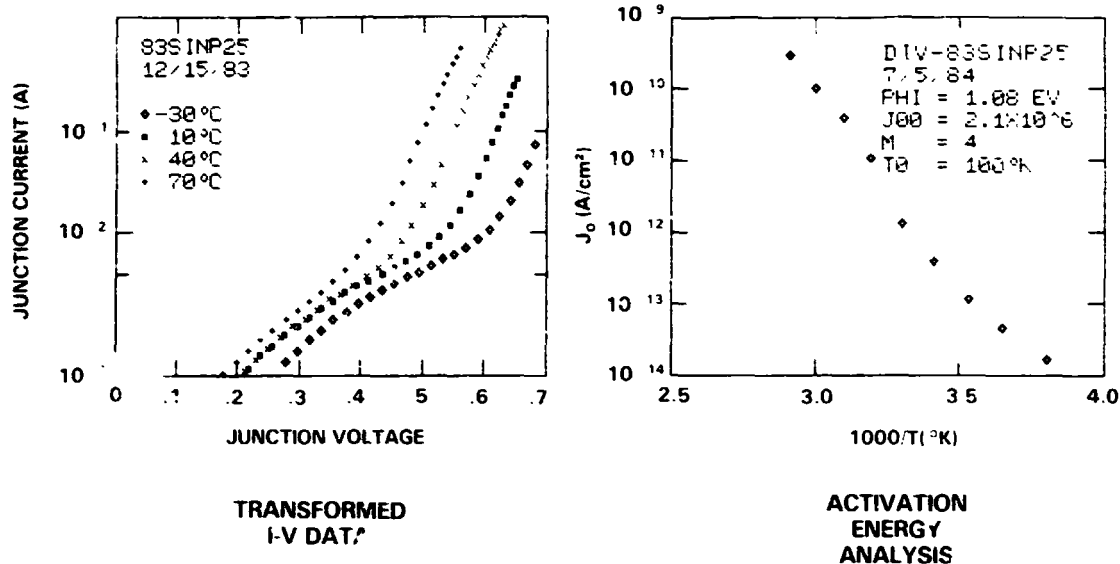


Figure 12. Current-Voltage Characteristics Of An MINP Cell Based On A Polished Substrate.

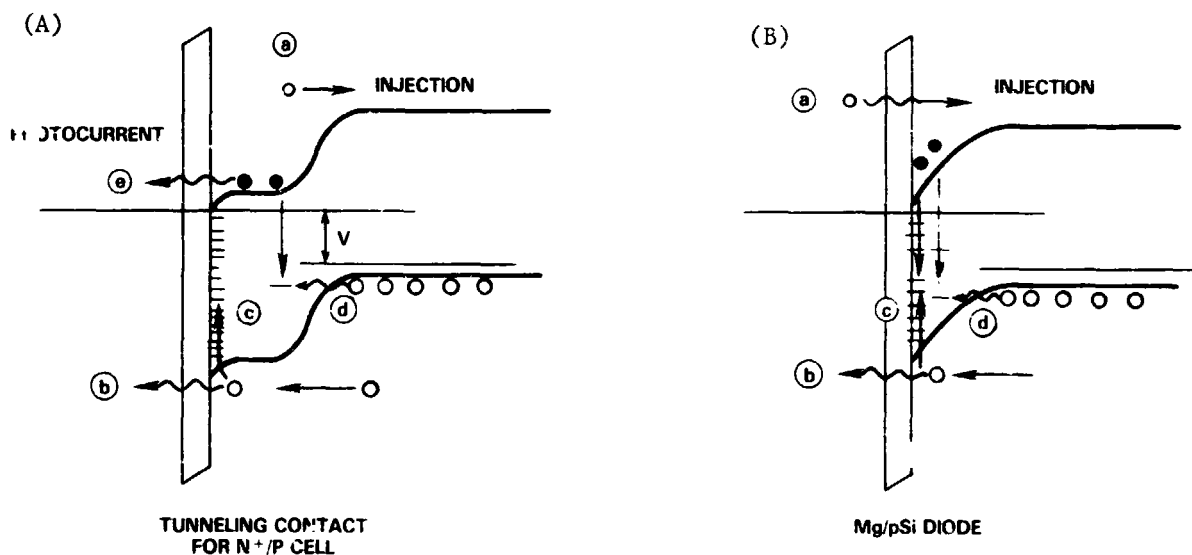


Figure 13. Electron Band Diagrams For Tunneling Contact On  $n^+$  Surface, And MIS Device On A P-type Substrate.



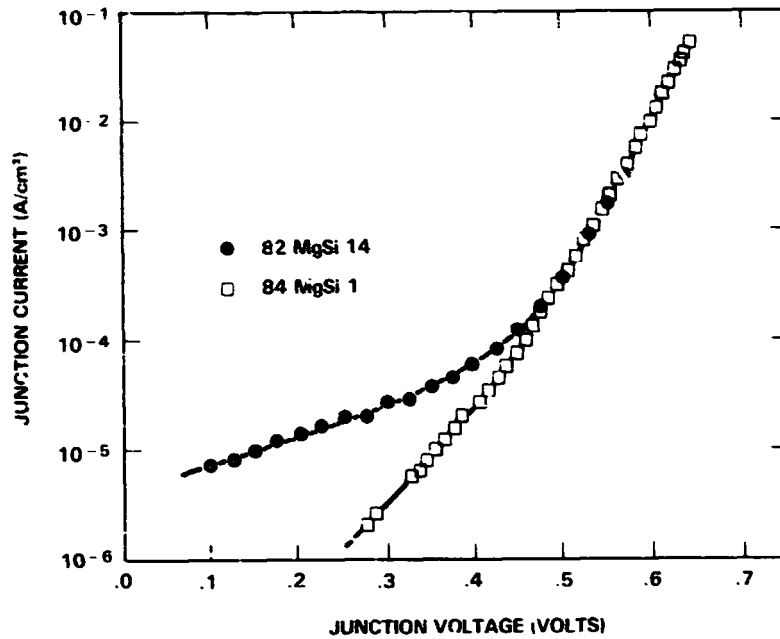


Figure 14. Current-Voltage Characteristics Of Mg/pSi MIS Devices Based On 0.2  $\Omega$ -cm Silicon.

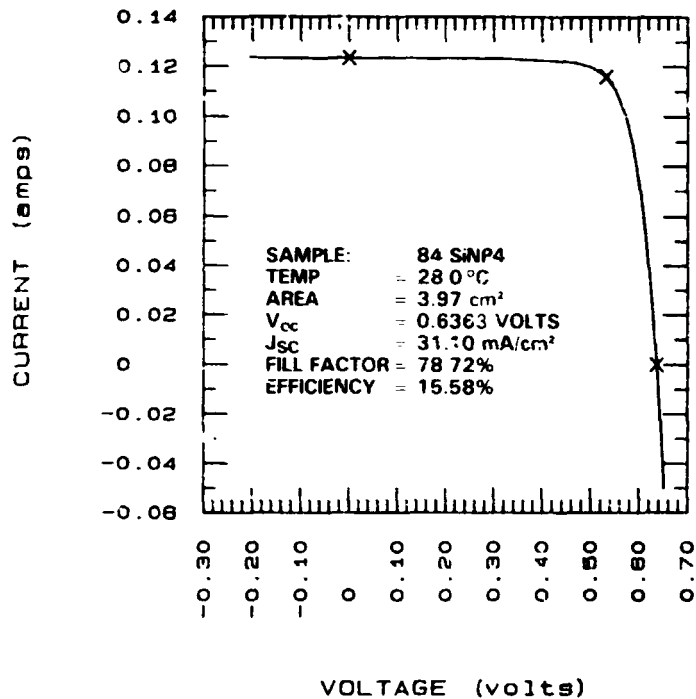


Figure 15. Illuminated Current-Voltage Characteristics Measured By SERI For MINP Cell With Polished Surface And SiO AR Layer.

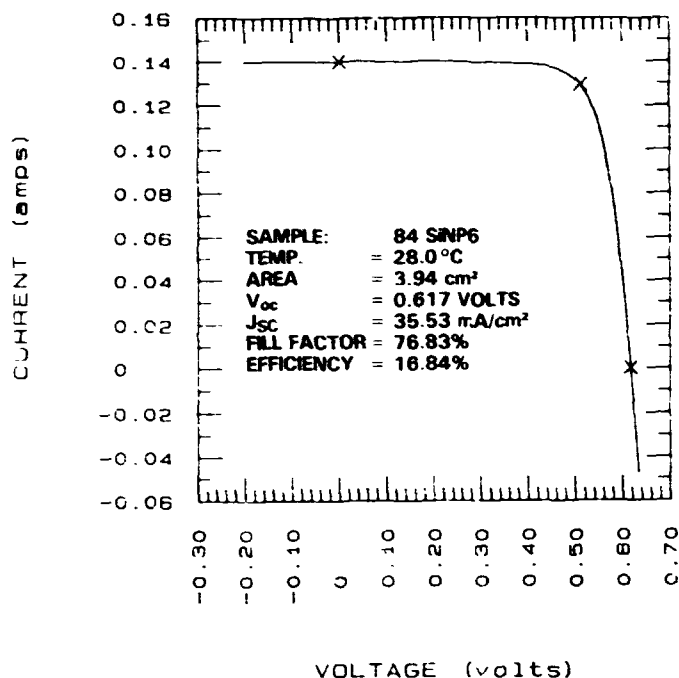


Figure 16 Illuminated Current-Voltage Characteristics Measured By SERI For MINP CELL With Textured Surface.

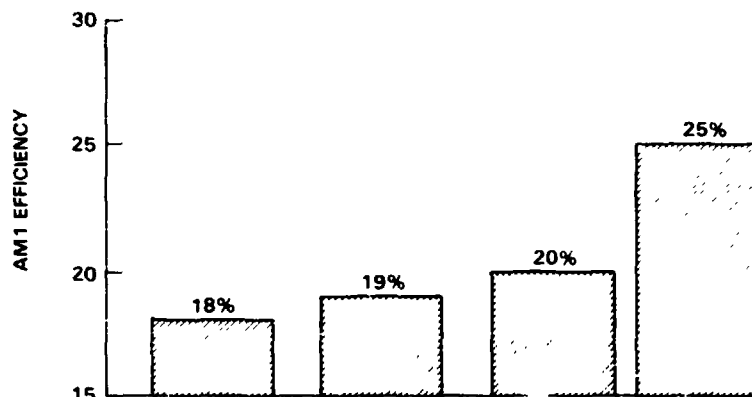
## PROJECTED PERFORMANCE

### TO ACHIEVE 20%

- MUST REDUCE  $J_{0E}$  BY DECREASING  $N_S$  AND  $S_p$
- NEED SLIGHT IMPROVEMENT IN L

### TO ACHIEVE 25%

- NEED F&P DIFFUSION LENGTH
- MUST REDUCE  $S_p$  TO  $10^2$
- WITH THESE VALUES OF L AND  $S_p$ ,  $J_0$  WILL BE DECREASED TO  $\approx 3 \times 10^{-14}$  A/cm<sup>2</sup>
- MUST USE DOUBLE AR WITH TEXTURED SURFACE OR WITH COMPLETE OPTICAL CONFINEMENT



$J_{sc}$ (mA/cm <sup>2</sup> )	36.0	36.0	36.7	40.9
$V_{oc}$ (mV)	630	650	670	720
FF	.794	.812	.820	.850
$J_0$ (A/cm <sup>2</sup> )	$1 \times 10^{-12}$	$4.5 \times 10^{-13}$	$2 \times 10^{-13}$	$3 \times 10^{-14}$
n-VALUE	1.0	1.0	1.0	1.0
$N_S$ (cm <sup>-3</sup> )	$6 \times 10^{19}$	$4 \times 10^{19}$	$2 \times 10^{18}$	$2 \times 10^{19}$
SURF REC VEL	$10^4$	$10^3$	$10^3$	$10^2$
DIFF LENGTH	150	150	200	500 (F&P)
GRID SHADOW	4%	4%	3%	2%
CELL THICKNESS	15 mils	15 mils	15 mils	10 mils
BACK SURF	Ohmic	Ohmic	BSF	BSF

Figure 17. Estimated Property Improvements For High Efficiency MINP Cells.

## DISCUSSION

SWANSON: How did you grow the thin oxides?

OLSEN: After we deposit aluminum to establish the back contact, a heat treatment at 500°C is carried out, and that process will grow a 20Å oxide.

SWANSON: Just from residual water, from the air?

OLSEN: Bill (Addis), why don't you comment on that?

ADDIS: The oxidation is carried out in a tube furnace.

SWANSON: Dry oxygen?

OLSEN: Yes.

SWANSON: Have you investigated different ways of forming the oxide and found whether any are better than others?

OLSEN: Not yet. We would like to try nitriding, and I have some thoughts on pursuing that further, but right now we have been going with the standard 20Å oxide.

SWANSON: Have you measured the contact resistance?

OLSEN: I think so. On the 0.3% area coverage, on a 2 x 2 solar cell,  $R_s$  is still below 0.1 ohm.

SWANSON: Doesn't seem good for concentrators.

OLSEN: Something seems to happen. It's strange; when the area goes down you get higher current density. The contact resistance goes down.

SWANSON: Did I read you correctly that you got a better  $J_0$  without the n layer under there than you did with the n layer? You said  $3 \times 10^{-13}$  (A/cm<sup>2</sup>).

OLSEN: No. That was for an MIS structure. Magnesium on p-type.

SWANSON: That is what I meant.

OLSEN: I think that is pertinent, mainly because it tells you something of the quality of the magnesium deposition and what it does to the p-type material. But it is a different situation, it appears, when you deposit onto an n-type surface. For a Mg/p-Si MIS diode, the value of  $3 \times 10^{-13}$  is approximately the theoretical value for  $J_0$ .

SWANSON: One would think you would want to take the n-layer out then, if it is--

OLSEN: Well, the problem with an MIS structure is the magnitude of photocurrent, which is too low. You just can't get adequate optical coupling, that is, transmission of the photons through the metal. Maybe something worth considering along the same lines is an inversion-layer cell. That is one without any doping done at all. That is something we have worked on in the past.

SWANSON: I sort of had the feeling that the phosphorus diffusion is not giving you the performance it could.

OLSEN: That's true. I think it is really hard to pin all this down. But I think it is clear that Green and his group have tailored their emitter to some degree and they have reduced the emitter recombination.

KEAVNEY: When you said you had 20 Å of oxide underneath the metal, I assume you measured that by ellipsometry.

OLSEN: That is right.

KEAVNEY: Do you have any ideas as to whether that is really 20 Å of oxide or whether there is an organic contamination throwing off the measurement?

OLSEN: The ellipsometry gives you 15 to 20 Å and it is not really clear what that means. You really have to couple that information with other information such as MIS current-voltage characterization. The MIS devices we have looked at are really high-quality ones. So that tells us that the interfacial layer is of high quality. Then, also, surface recombination effects in the solar cells themselves seem to be reasonable.

WOLF: It seems to me that Marty Green told us at the Photovoltaic Specialists Conference that his 19% cell was not an MINP structure but a dot contact structure. He had a new acronym for it too, PEST or something like that.

OLSEN: A dot contact cell, that is just what we made too. That simply means that you put slots in the thermal oxide on the surface, and the collector grid only contacts a small area. But the question is: what is the nature of his contact at the interface?

WOLF: That is right. That is what I thinking.

OLSEN: He didn't think it was MIS anymore?

WOLF: That was my impression.

OLSEN: I wouldn't argue about it. They do sinter, like the standard procedure. I think, in theory, titanium can be used as an MIS contact. It just may be very difficult to keep the oxygen out of it and get a decent contact. Maybe that is why you have to sinter. We have stuck with magnesium because it is not limiting us at this point and we haven't been motivated to change. But we are considering changing, because the use of magnesium impacts other processes. So we will move to try titanium as well, eventually.

WOLF: Another thing. I was a little surprised that you took the band gap as 1.2 eV. That is the zero Kelvin number. Really it is, at room temperature, more like 1.1.

OLSEN: I know that. But if you look at the band gap expression versus temperature, it is 1.2, minus some constant, times temperature. The constant times temperature divided by  $kT$  gives you an  $e^{-\text{constant}}$  so that goes out into the pre-exponential number.

WOLF: So that is where you put it?

OLSEN: Yes. I hope that was clear to others. The band gap, I agree is 1.12, but it is the temperature dependence that I wanted to account for. An activation analysis gets 1.2 minus the bandgap narrowing.

QUESTION: (Inaudible; concerning the use of magnesium.)

OLSEN: No. We can't heat treat it. We haven't used titanium, but Green, for example, does heat treat at something like 450°C.

WOLF: I thought we might have some questions with respect to all the papers together, and overall comments on the afternoon session -- even the morning session -- before we break up. One comment I would like to make: I feel that what we really all sat and listened to this afternoon was perhaps more how do we model, what do we learn out of the modeling, and how does what we are doing actually relate to what we calculate? Rather than, really, concepts on how to get higher efficiency. So it seems to me it was more really modeling results and what did we learn from the modeling. I don't know whether that is challenging enough for more discussion or not. We certainly, some of us, use low-level modeling and get up to some point with that, and then comes high-level modeling beyond that. We will hear more about modeling tomorrow in any case.

LESK: I am still confused. In the back contact you had only BSF. Specifically, what is the difference between ohmic and a BSF back-surface contact?

OLSEN: Well, BSF refers to back-surface field. An adequate BSF yields a surface recombination velocity of zero.

LESK: I am not sure I got that right. In BSF -- in your equation you put  $S = 0$  -- that means BSF?

OLSEN: That's right.

LESK: For ohmic,  $S$  is infinity but if you are maintaining the equilibrium in order to carry concentration to the back contact, that means ohmic. Is that the way it is used?

OLSEN: Yes. The point is with low-cost silicon sheet material, the use of a BSF makes little difference to current. But, if you increase the lifetime, then a BSF can have a significant impact on photocurrent.

WOLF: Are these things we are looking at here really all the approaches we can pursue to get to a higher efficiency? Are there things we should be looking at in addition? Does what we have been talking about really exhaust the methods available at this time?

SPITZER: I wanted to mention a few things. On the idea of how to improve efficiency, I think some people referred to this. We are neglecting lots of current. The theoretical limit is 44 and if you tune up the base diffusion length, that current could easily be raised from 36, which most people are achieving, to about 38 with a back-surface reflector and diffusion length of 300 micrometers, which doesn't seem that hard to do. And, say, with 38 milliamps/m<sup>2</sup> and a voltage of 660, with a fill factor of 0.8, that would be 20%. So I think some attention should be addressed to improving J<sub>sc</sub>.

WOLF: It seems essentially that everybody who is working on high-efficiency cells sees how he can make the next step to get 20%. It seems that this is just about imminent. I think the big question after that becomes, how do we get to 22 or 23, and do we really have to get the trap densities down, or are there other remedial steps we can be doing to get the efficiencies up? Have we really exhausted all the cell-design approaches to a large enough degree for this next step?

SWANSON: I think the goal of 15% modules is rather modest in view of the 19% cells that are already being made.

WOLF: No.

SWANSON: We are talking efficiency, not getting cost down. But I think if you want to go to the 15% range, you should very seriously consider the Yablonoich design, which in my opinion has the potential of 25%.

WOLF: He combines again a number of the things we have been discussing, and also Dick Swanson. How to get high lifetime is one of his key aspects. How to get the lifetime up, how to get the surface recombination velocity down, use a wider band-gap material on one side, etc.

DYER: I have been out of this field for a number of years, but what are the difficulties with that overlap approach that someone mentioned earlier?

WOLF: It is called the shingling of cells.

DYER: What is the difficulty with that? You mentioned it, but I don't see any --

WOLF: Well, I don't think I mentioned that by saying there was a difficulty with it. It has been used for a long time in making submodules for space arrays. I guess it has given a certain amount of inflexibility within the array. One other approach was to make flexible interconnects, but still overlapping as far as individual soldering together is concerned.

DYER: Does it come out so it is not worth it, is what I am after.

WOLF: No.

DYER: Is it such that it is very successful and you can say, Well, we can gain back all that we devote to metallization, or is it not worth it?

WOLF: Well, you have no contact shading at all on the front, so you have all active surface that way. I see a little bit of a problem if the whole cell length is only 2 millimeters and then you overlap. You get quite a bit out of the horizontal with the whole thing, but I don't think that is too much of a problem area. You can somehow adjust for it again. No. I don't see a major problem with it. I guess from a manufacturing viewpoint it might be tough to make so many very small little devices and then assemble them into a bigger thing. It might give extra cost. But that's not fundamental. Somehow you can imagine some nice assembly machine that handles all these tiny little parts and makes a bigger thing out of it.